

# The Flavour-Changing Neutral Currents Decay $t \rightarrow Hq$ at ATLAS Experiment

**Leila Chikovani**

Institute of Physics of the Georgian Academy of Sciences

**Tamar Djobava**

High Energy Physics Institute, Tbilisi State University

**Tamaz Grigalashvili**

Institute of Physics of the Georgian Academy of Sciences

## ABSTRACT

The sensitivity of the ATLAS experiment to the top-quark rare decay via flavour-changing neutral currents  $t \rightarrow Hq$  ( $q$  represents  $c$  and  $u$  quarks) has been studied at  $\sqrt{s}=14$  TeV in the decay mode of  $t\bar{t} \rightarrow HqWb \rightarrow WW^*q, Wb \rightarrow l\nu l\nu j, l^\pm \nu b$ , ( $l=e, \mu$ ).

The Standard Model backgrounds  $t\bar{t}$ ,  $t\bar{t}H$ ,  $WZ$  and  $WH$  have been analysed. The signal and backgrounds were generated via PYTHIA 5.7 and simulated and analysed using ATLFAST 2.51. A branching ratio for  $t \rightarrow Hq \rightarrow WW^*q$  as low as  $2.0 \times 10^{-3}$  for  $m_H = 150$  GeV and  $2.1 \times 10^{-3}$  for  $m_H = 160$  GeV could be discovered at the  $5\sigma$  level with an integrated luminosity of  $100 \text{ fb}^{-1}$ .

# 1 Introduction

We study the sensitivity of the ATLAS experiment to the branching ratio of the top-quark rare decay via flavour changing neutral currents (FCNC)  $t \rightarrow Hq$  ( $q = u, c$ ), where  $H$  is the Standard Model Higgs ( $m_t = 175$  GeV,  $M_Z \leq M_H \leq 2M_W$ ). The SM prediction for the branching ratio is of order  $\text{Br}(t \rightarrow H_{SM}q) \approx 0.9 \cdot 10^{-13} (4 \times 10^{-15})$  for  $m_H = 100 (160)$  GeV [1]. Thus, an observation of this decay mode at the LHC, would provide a clear signal of new physics beyond the SM, such as new dynamical interactions of top quark, multi-Higgs doublets, exotic fermions or other possibilities [2,3,4,5]. The recent theoretical estimations of branching is  $\text{Br}(t \rightarrow Hq) \sim 10^{-5} \div 10^{-4}$  [5]. We consider the following process  $t\bar{t} \rightarrow HqWb \rightarrow WW^*q, Wb \rightarrow l\nu l\nu j, l^\pm \nu b$ , ( $l = e, \mu$ ) for Higgs masses  $m_H = 150$  GeV and  $m_H = 160$  GeV in the leptonic decay topology of W bosons since in this mass range  $H \rightarrow WW^*$  is the dominant decay mode.

## 2 Monte Carlo Event Generation

It is known, that the dominant mechanism of top quark production at the LHC is  $t\bar{t}$  pair production via  $gg, q\bar{q} \rightarrow t\bar{t}$ .

For the implementation of the  $t \rightarrow Hq$  process into PYTHIA 5.7 all individual decay channels of the top quark were switched off, except two decay modes  $t \rightarrow Wb$  and  $t \rightarrow Ws$ . The last one was replaced by the decay of the  $t \rightarrow Hq$ , by replacing of  $W$  by  $H$  and  $s$  by  $c(u)$ .

The  $t\bar{t}$  events have been generated by PYTHIA 5.7 at  $\sqrt{s} = 14$  TeV,  $m_{top} = 175$  GeV for two masses of Higgs  $m_H = 150$  GeV and  $m_H = 160$  GeV with proton structure function CTEQ2L. Initial and final state QED and QCD (ISR, FSR) radiations, multiple interactions, fragmentations and decays of unstabled particles were enabled. The total cross-section for  $t\bar{t}$  production was assumed to be  $\sigma_{t\bar{t}} = 833$  pb (NLO prediction) [6].

The following SM backgrounds have been considered for above mentioned process:

- $t\bar{t} \rightarrow WbWb \rightarrow l^+\nu bl^-\bar{\nu}b$
- $t\bar{t}H \rightarrow W^+bW^-\bar{b}, WW^* \rightarrow l^+\nu b, l^-\bar{\nu}b, l^+\nu l^-\bar{\nu}; l^\pm \nu b, jjb, l^+\nu l^-\bar{\nu}; l^+\nu b, l^-\bar{\nu}b, jjl\nu$
- $WZ \rightarrow l^\pm \nu l^+ l^- + X$
- $WH \rightarrow l^\pm \nu WW^* \rightarrow l^\pm \nu, l^+\nu l^-\bar{\nu} + X$

In case of  $t\bar{t}$  background the third lepton originates from a semileptonic  $b$  -decay.

All backgrounds were generated by PYTHIA 5.7.

The performance of the ATLAS detector was simulated using the fast simulation package ATLFAST 2.51 [7], which uses parametrizations of the detector resolution functions. High luminosity (KEYLUM=2) option has been invoked.

The b tagging perfomance was simulated assuming the nominal efficiencies of  $\epsilon_b = 50\%$ ,  $\epsilon_c = 10\%$ ,  $\epsilon_j = 1\%$ . The lepton identification efficiency is  $\epsilon^l = 0.9$ . The branching ratios of  $H \rightarrow WW^*$  decays have been estimated by the Fortran code HDECAY [8].  $\text{Br}(H \rightarrow WW^*) = 0.6852$  ( $0.9160$ ) for  $m_H = 150$  GeV ( $160$  GeV).

### 3 Event Analysis

The experimental signature of  $t\bar{t} \rightarrow HqWb \rightarrow WW^*j, Wb \rightarrow l\nu l\nu j, l\nu b$  includes three isolated leptons, missing transverse momentum due to neutrinos, one b-jet and an additional light jet.

The leptonic decay mode of  $W$  bosons have been considered for the final topology of backgrounds.

Numbers of generated and expected events of signal and backgrounds for two masses of Higgs  $m_H = 150$  GeV and  $m_H = 160$  GeV are presented in Tables 1÷2. In order to discriminate the signal from the background processes, the following preselection cuts have been applied:

- At least three isolated charged leptons (electrons with  $P_T > 5$  GeV,  $|\eta| < 2.5$  and muons with  $P_T > 6$  GeV,  $|\eta| < 2.4$ ) are required. Lepton isolation criteria in terms of the distance from other clusters  $\Delta R > 0.4$  and of maximum transverse energy deposition in cells  $E_T < 10$  GeV in a cone  $\Delta R=0.2$  around the leptons were applied.
- Events without at least two jets with  $P_T^{jet} > 15$  GeV and  $|\eta| < 5$ , are rejected.

The preselection cuts reduce backgrounds approximately from 2% up to 14%, meanwhile  $\sim 50\%$  of signal events are survived.

Then a kinematical cut was applied, requiring the presence of three isolated charged leptons with high  $P_T^l > 30$  GeV. This cut certainly includes the presence of one opposite charged lepton in event. Such requirement affects (reduces) significantly  $t\bar{t}$  dangerous background, while keeping still a significant fraction of the signal.

The next requirement of the missing transverse momentum in event with  $P_T^{miss} > 45$  GeV is a powerful cut for reduction of  $WZ$  background (see Fig. 1), though other backgrounds are less sensitive to this cut. One can see from Fig. 1, that  $t\bar{t}H$  background is extended to larger values of  $P_T^{miss}$  than other backgrounds due to four neutrinos in  $t\bar{t}H$ .

We demand the presence of at least two jets with high  $P_T^{jet} > 30$  GeV in the pseudorapidity region  $|\eta^{jet}| < 2.5$ , which satisfy the following isolation conditions:  $\Delta R_{jj} > 0.4$  (jet-jet isolation) and  $\Delta R_{lj} > 0.4$  (lepton-jet isolation). Among the isolated high  $P_T$  jets is required the presence at least of one tagged b-jet. This cut significantly suppresses  $WZ$  background and vanishes  $WH$ .

For the dilepton (coming from  $H$  decay) mass  $m_{ll}$  reconstruction it have been required opposite charged lepton pairs with  $\Delta\phi < 1.0$  ( the opening angle between the two leptons in the transverse plane, measured in rad.),  $|\Delta\eta| < 1.5$  ( the absolute values of the pseudorapidity difference between the two leptons) and an invariant dilepton mass smaller than 80 GeV [9]. The small angular separation between leptons in signal events results from the opposite spin orientation of the  $W$  pair originating from the decay of the scalar Higgs boson [10]. The discrimination between the signal and the most important backgrounds ( $t\bar{t}$ ,  $t\bar{t}H$ ) is shown for the pseudorapidity difference  $|\Delta\eta|$  and the azimuthal difference  $\Delta\phi$  between the two leptons, respectively, in Figures 2 and 3. One can see, that these cuts sufficiently reduce  $t\bar{t}$  background and  $WZ$  background is vanished (see Tables 1÷2).

In Fig. 4 are presented the dilepton invariant mass  $m_{ll}$  distributions for signal and  $t\bar{t}H$ ,  $t\bar{t}$  background events for a Higgs mass of 160 GeV. The solid histogram is for best combinations of dilepton pairs for signal and dashed histogram is for Higgs decay product leptons at parton level. The best combinations of  $ll$  invariant mass is defined as the closest values to the mean of the  $ll$  dilepton mass distribution of signal at parton level. One can see a good agreement between parton level and best combinations of dilepton pairs. The  $t\bar{t}$  and  $t\bar{t}H$  events are reduced by  $\approx 50\%$ .

Then the kinematical cuts have been applied on the two invariant masses of:

- a)  $m_{llj} < 110$  GeV with light jets  $P_T > 30$  GeV and
- b)  $m_{lb} < 140$  GeV with  $P_T^{bjet} > 40$  GeV.

In Fig. 5 are presented the invariant  $llj$  mass distributions for a Higgs mass of 160 GeV for the best combinations of signal (solid histogram), for  $t\bar{t}H$  background (dotted histogram),  $t\bar{t}$  background (dashed-dotted histogram) and invariant mass of  $llq$  for signal at parton level (dashed histogram). One can see an agreement between parton level and the best combinations of  $llj$ .

The sequence of  $m_{llj} < 110$  GeV and  $m_{lb} < 140$  GeV cuts significantly suppresses the  $t\bar{t}H$  and  $t\bar{t}$  backgrounds and other remained backgrounds are vanished.

In Fig. 6 are presented the invariant  $lb$  mass distributions for a Higgs mass of 160 GeV for the best combinations of signal (solid histogram), for  $t\bar{t}H$  background (dotted histogram),  $t\bar{t}$  background (dashed-dotted histogram) and invariant mass of  $lb$  for signal at parton level (dashed histogram). One can see an agreement between parton level and the best combinations of  $lb$  for the signal and remained backgrounds.

The acceptances and the expected rates for signal and background events after applying all above mentioned kinematical cuts are summarised in Tables 1÷2 for  $m_H=150$  and 160 GeV. The sensitivities to  $\text{Br}(t \rightarrow Hq)$  have been calculated similarly as in [11]. Table 3 summarizes the branching ratios for the  $t \rightarrow Hq \rightarrow WW^*q$  decay at the different levels of applied cuts. One can see from Table 3, that  $\text{Br}(t \rightarrow Hq)$  as low as  $2.0 \times 10^{-3}$  could be discovered at the  $5\sigma$  level for  $m_H=150$  GeV and as low as  $2.1 \times 10^{-3}$  for  $m_H=160$  GeV with an integrated luminosity of  $100 \text{ fb}^{-1}$ .

## 4 Conclusions

We have studied the ATLAS sensitivity to the FCNC top quark rare decay  $t \rightarrow Hq$  ( $q = u, c$ ) with  $H \rightarrow WW^*$  at  $\sqrt{s} = 14$  TeV for an integrated luminosity of  $100 \text{ fb}^{-1}$ . The results demonstrate that, a branching ratio as low as  $2.0 \times 10^{-3}$  could be discovered at the  $5\sigma$  level for  $m_H=150$  GeV and  $2.1 \times 10^{-3}$  for  $m_H=160$  GeV, respectively.

## 5 Acknowledgements

We are very thankful to M.Cobal, J.Parsons, D.Pallin and E.Richter-Was for very interesting and important discussions.

The work was supported in part by Georgian Academy of Sciences grant 2.16.04.

## References

- [1] B.Mele, S.Petrarca, A.Soddu, Phys.Lett. B435 (1998) 401, hep-ph/9805498;  
G.Eilam, J.Hawett and A.Soni, Phys.Rev. D59 (1999) 039901, Erratum
- [2] G.Eilam, J.Hawett and A.Soni, Phys.Rev. D44 (1991) 1473
- [3] T.Han, R.Peccei and X.Zhang, Nucl.Phys. B454 (1995) 527
- [4] B.Grzadkowski, J.Gunion and P.Krawczyk, Phys.Lett. B268 (1991) 106;  
M.Luke and M.Savage, Phys.Lett. B307 (1993) 387;  
G.Couture, C.Hamzaoui and M. Konig, Phys. Rev. D52 (1995) 1713
- [5] J.Guasch, in \*Barcelona 1997, Quantum effects in the minimal supersymmetric standard model, p. 256; hep-ph/9710267;  
J.Guasch and J.Sola, Nucl. Phys. B562 (1999) 3; hep-ph/9906268
- [6] R.Ronciani et al., Nucl.Phys. B529 (1998) 424
- [7] E.Richter-Was, D.Froidevaux and L.Poggioli, ATLAS Internal Note ATL-PHYS-98-131, 1998
- [8] A.Djouadi, J.Kalinowski and M.Spira, DESY 97-079, IFT-96-29, PM-97-4; hep-ph/9704448, 1997
- [9] Detector and Physics Performance, Technical Desigh Report, vol. II, CERN/LHCC/99-15, ATLAS TDR 15, p.705, 1999
- [10] C.A. Nelson, Phys.Rev. D37 (1988) 1220
- [11] L.Chikovani and T.Djobava, hep-ex/0008010, 2000

Description of Cuts	$t \rightarrow Hq$ Signal		Background Processes							
			$t\bar{t}H$		$WH$		$t\bar{t}$		$WZ$	
	Nevt	Eff (%)	Nevt	Eff (%)	Nevt	Eff (%)	Nevt	Eff (%)	Nevt	Eff (%)
Nevt gen.	10.4K		110K		300K		4M		200K	
Expect. events			12950		430		3.9M		39040	
Preselection	5012	48.00	395	3.05	56	13.07	93611	2.41	3552	9.10
$P_T^{mis} > 45 \text{ GeV}$										
$P_T^l > 30 \text{ GeV}$										
$P_T^{jet} > 30 \text{ GeV}$	249	2.39	48	0.38	0	$5.13 \times 10^{-2}$	152	$3.91 \times 10^{-3}$	5	$1.28 \times 10^{-2}$
$N_{b-jet} > 0$										
$m_{ll} < 80 \text{ GeV}$										
$\Delta\eta < 1.5$	186	1.79	22	0.17	0	$4.03 \times 10^{-2}$	38	$9.78 \times 10^{-4}$	0	$1.00 \times 10^{-3}$
$\Delta\phi < 1.0$										
$t \rightarrow Hq$										
$m_{llj} < 110 \text{ GeV}$	87	0.84	6	$5.09 \times 10^{-2}$	0	$7.30 \times 10^{-3}$	7	$1.80 \times 10^{-4}$	0	$5.00 \times 10^{-4}$
$P_T^j > 30 \text{ GeV}$										
$t \rightarrow Wb$										
$m_{lb} < 140 \text{ GeV}$	78	0.75	6	$4.64 \times 10^{-2}$	0	$6.70 \times 10^{-3}$	3	$7.72 \times 10^{-5}$	0	$5.00 \times 10^{-4}$
$P_T^b > 40 \text{ GeV}$										

Table 1: The numbers of events and efficiencies (%) of kinematic cuts applied in sequence for the signal and backgrounds for  $m_H = 150 \text{ GeV}$  (are not multiplied on the lepton identification efficiency ( $\epsilon^l$ )<sup>3</sup>). The numbers of events after cuts for backgrounds are presented according to the expected events.

Description of Cuts	$t \rightarrow Hq$ Signal		Background Processes							
			$t\bar{t}H$		$WH$		$t\bar{t}$		$WZ$	
	Nevt	Eff (%)	Nevt	Eff (%)	Nevt	Eff (%)	Nevt	Eff (%)	Nevt	Eff (%)
Nevt gen.	8.8K		32.8K		15K		4M		200K	
Expect. events			15020		480		3.9M		39040	
Preselection	3943	45.00	475	3.16	66	13.70	93611	2.41	3552	9.10
$P_T^{mis} > 45 \text{ GeV}$										
$P_T^l > 30 \text{ GeV}$										
$P_T^{jet} > 30 \text{ GeV}$	218	2.48	76	0.51	0	$5.33 \times 10^{-2}$	152	$3.91 \times 10^{-3}$	5	$1.28 \times 10^{-2}$
$N_{b-jet} > 0$										
$m_{ll} < 80 \text{ GeV}$										
$\Delta\eta < 1.5$	170	1.93	35	0.24	0	$4.67 \times 10^{-2}$	38	$9.78 \times 10^{-4}$	0	$1.00 \times 10^{-3}$
$\Delta\phi < 1.0$										
$t \rightarrow Hq$										
$m_{llj} < 110 \text{ GeV}$	60	0.68	12	$8.54 \times 10^{-2}$	0	$6.70 \times 10^{-3}$	7	$1.80 \times 10^{-4}$	0	$5.00 \times 10^{-4}$
$P_T^j > 30 \text{ GeV}$										
$t \rightarrow Wb$										
$m_{lb} < 140 \text{ GeV}$	59	0.67	11	$7.62 \times 10^{-2}$	0	$5.10 \times 10^{-3}$	3	$7.72 \times 10^{-5}$	0	$5.00 \times 10^{-4}$
$P_T^b > 40 \text{ GeV}$										

Table 2: The numbers of events and efficiencies (%) of kinematic cuts applied in sequence for the signal and backgrounds for  $m_H = 160 \text{ GeV}$  (are not multiplied on the lepton identification efficiency ( $\epsilon^l$ )<sup>3</sup>). The numbers of events after cuts for backgrounds are presented according to the expected events.

Cuts	Sensitivity to $\text{Br}(t \rightarrow Hq)$	
	$m_H = 150 \text{ GeV}$	$m_H = 160 \text{ GeV}$
$t \rightarrow Hq$ $m_{llj} < 110 \text{ GeV}, P_T^j > 30 \text{ GeV}$	$2.19 \times 10^{-3}$	$2.43 \times 10^{-3}$
$t \rightarrow Wb$ $m_{lb} < 140 \text{ GeV}, P_T^b > 40 \text{ GeV}$	$2.03 \times 10^{-3}$	$2.12 \times 10^{-3}$

Table 3: Summary of the results at  $L = 100 \text{ fb}^{-1}$ .

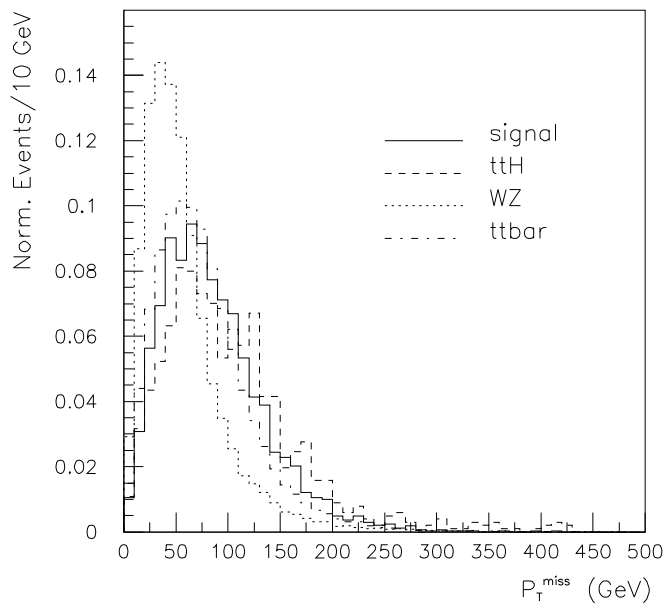


Figure 1: The  $P_T^{\text{miss}}$  distributions for signal events with  $m_H = 160$  GeV and  $t\bar{t}H$ ,  $t\bar{t}$  and  $WZ$  backgrounds. All distributions are normalised to unity.

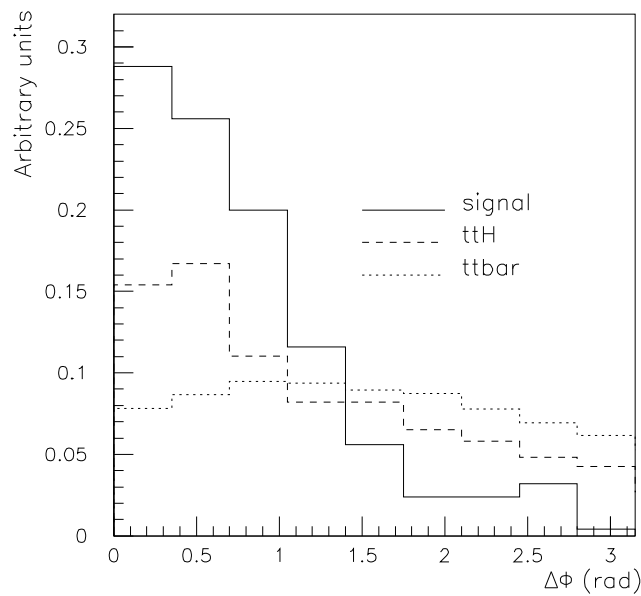


Figure 2: Difference in azimuth between the two leptons for signal events with  $m_H = 160$  GeV and  $t\bar{t}$  and  $t\bar{t}H$  backgrounds. All distributions are normalised to unity.

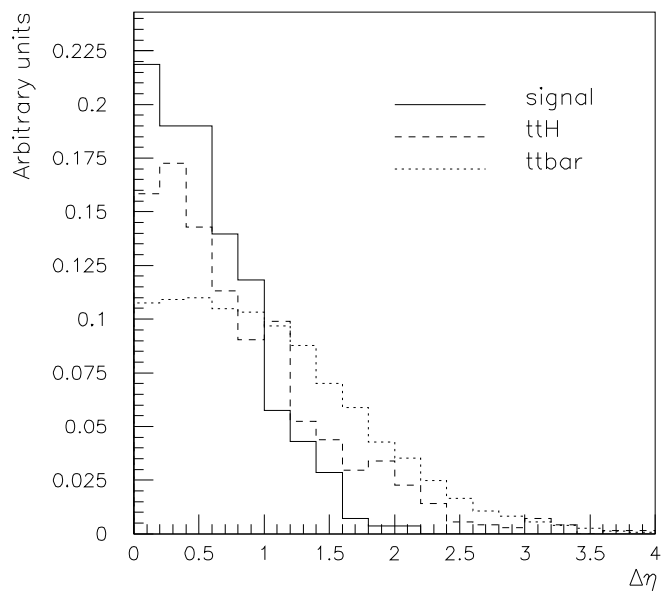


Figure 3: The absolute values of the pseudorapidity difference between the two leptons for signal events with  $m_H = 160$  GeV and  $t\bar{t}$  and  $t\bar{t}H$  backgrounds. All distributions are normalised to unity.

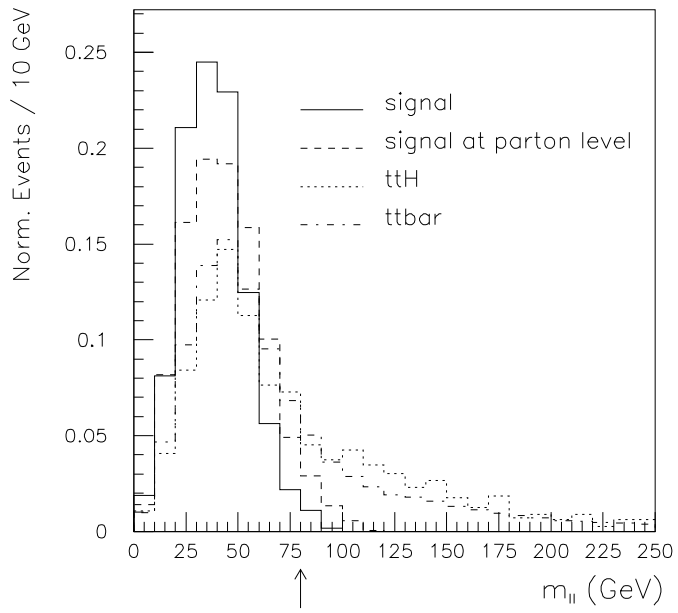


Figure 4: Invariant  $ll$  mass distributions for the signal and background events: the solid histogram for the best combinations of signal, the dashed histogram for signal at parton level, the dotted histogram for  $t\bar{t}H$  background, the dashed-dotted histogram for  $t\bar{t}$ . The arrow indicates the value of cut on dilepton mass.

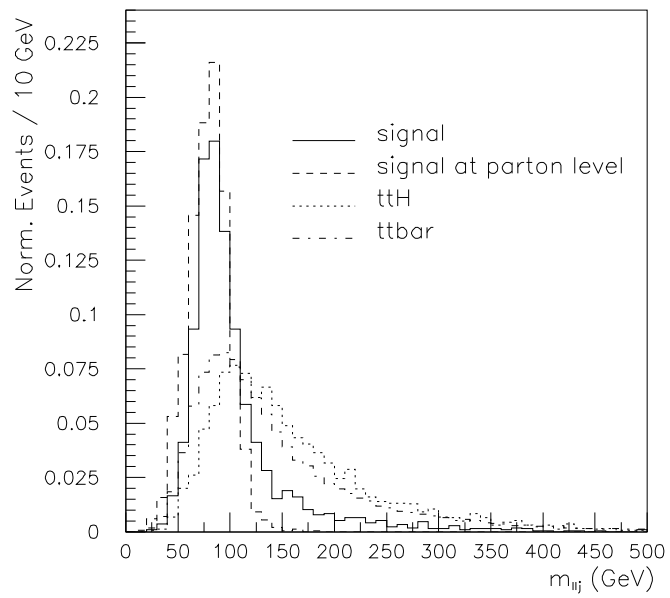


Figure 5: Invariant  $llj$  mass distributions for the signal and background events: the solid histogram for the best combinations of signal, the dashed histogram for signal at parton level, the dotted histogram for  $t\bar{t}H$  background, the dashed-dotted histogram for  $t\bar{t}$ .

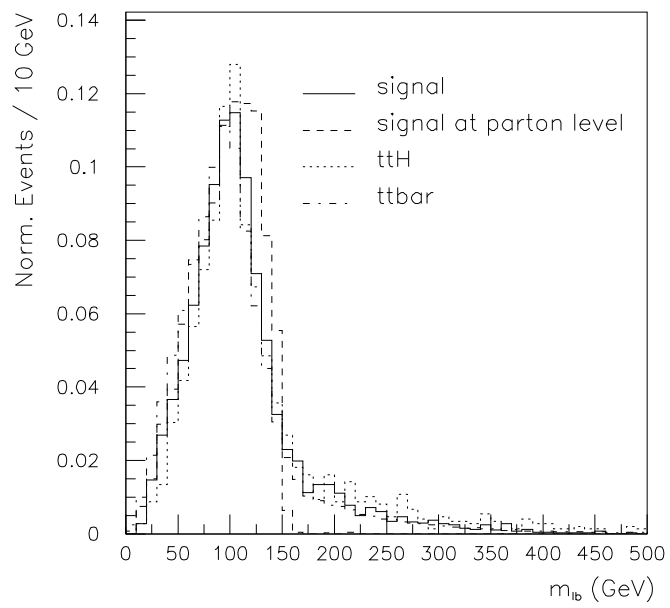


Figure 6: Invariant  $lb$  mass distributions for the signal and background events: the solid histogram for the best combinations of signal, the dashed histogram for signal at parton level, the dotted histogram for  $t\bar{t}H$  background, the dashed-dotted histogram for  $t\bar{t}$ .